Journal of Solid State Electrochemistry (2018) 22:2703–2714
https://doi.org/10.1007/s10008-018-3981-4

ORIGINAL PAPER

The charging-discharging behavior of the lead-acid cell with electrodes based on carbon matrix

Andrzej Czerwiński[1,2,3] · Justyna Wróbel[4] · Jakub Lach[2] · Kamil Wróbel[2] · Piotr Podsadni[5]

Received: 5 March 2018 / Revised: 27 April 2018 / Accepted: 29 April 2018 / Published online: 9 May 2018

Abstract

Reticulated vitreous carbon (RVC) plated electrochemically with a thin layer of lead was investigated as a carrier and current collector material for the positive and negative plates for lead-acid batteries. Flooded 2 V single lead-acid cells, with capacities up to 46 Ah, containing two positive and two negative plates were assembled and subjected to charge/discharge cycling tests, self-discharge characterization and Peukert's dependences determination. They could retain 72% of discharge capacity after 12 months of storage in room temperature and showed similar performance to a standard cell during cycle life test. A 2-V cell using a carbon material with higher conductivity than RVC was also constructed. It showed improved performance under higher current discharges, comparable to standard lead-acid batteries. Additional cycling tests were performed on a complete 12-V RVC-based battery. It completed almost three times the number of cycles of lead-acid batteries with standard current collectors. Obtained results are promising and show that application of a conducting porous carbon as a carrier and current-collector will significantly increase the specific capacity of the lead-acid battery and self-discharge characterization and cycling charging–discharging battery durability.

Keywords Lead-acid battery · Current collectors · Reticulated vitreous carbon · Energy storage

Introduction

Lead-acid batteries were invented about 160 years ago and evolved considerably over the years, but they are still one of the most widely used secondary batteries. The worldwide battery market for lead-acid batteries was around 18.5 billion US$ in 2010 [1]. It is well known that one of the main reasons for a relatively low specific capacity and energy of lead-acid batteries is the low utilization efficiency of the active mass in conjunction with the heavy weight of a conventional grid [2]. Lead electrodes constitute about 21% of total weight of the typical lead-acid car battery [3]. Recent research has shown that the use of lightweight carbon materials as a current collector and an active material support is helpful with respect to this problem. Many of the studies demonstrated light weight conductive porous grids made from reticulated vitreous carbon (RVC), carbon/graphite foams, or carbon honeycomb. The idea of porous glassy carbon application, especially RVC, in lead-acid battery construction has been first described by Czerwinski in a patent submitted in 1992 [4], as well as presented at the LABAT 96 Conference [5]. This idea was further described by his Warsaw University group in many patents and papers [6–13]. Das et al. [14] demonstrated the electrochemical behavior of graphite covered with lead in the perspective of application in lead-acid battery. Few years later, Snaper [15] described in the patent the use of reticulated current collectors' structures for battery applications. Gyenge et al. also adopted lightweight current collector for the construction of lead-acid batteries and investigated RVC electroplated with a Pb-Sn alloy as alternative for the

✉ Andrzej Czerwiński
aczerw@chem.uw.edu.pl

1 Faculty of Chemistry, University of Warsaw, Pasteura 1, 02-093 Warsaw, Poland

2 Industrial Chemistry Research Institute, Rydygiera 8, 01-793 Warsaw, Poland

3 Faculty of Chemistry, Biological and Chemical Research Centre, University of Warsaw, Żwirki i Wigury 101, 02-089 Warsaw, Poland

4 Division of Elastomers and Rubber Technology, Institute for Engineering of Polymer Materials and Dies, Harcerska 30, 05-820 Piastów, Poland

5 Department of Drug Technology and Pharmaceutical Biotechnology, Medical University of Warsaw, Banacha 1, 02-097 Warsaw, Poland

conventional grid battery [16–19]. Jang et al. [20] evaluated the electrochemical stability of the graphite foams as current collector materials to replace lead alloys. Chen et al. [21–24] demonstrated in a series papers small electrodes based on pitch-based carbon foam. Kelley and co-workers [25–27] proposed carbon foams as possible current collectors for lead-acid batteries described in patents applied by the start-up company Firefly Energy Inc. and Caterpillar Inc. Kirchev et al. [28–30] studied the carbon honeycomb grids as innovative alternative to the classical grids. The usual strategy to employ the lightweight porous carbon materials is to electroplate it with a lead or lead alloy coating. There are also several reports on the substitution of the lead alloy cast gird with a lead-foam grid [31–34].

One important aspect of batteries is their self-discharge, which leads to a capacity loss with time. The first report about the effect of self-discharge reactions on the lead-acid battery was published in 1882 [35]. The self-discharge phenomena are well defined; they are caused by the electrochemical reactions between the active materials in the plates, the electrolyte, the current collector, the separator, and other components in the cell or by the ohmic leakage currents [36]. The manufacture of lead-acid cells demands careful attention, since there are many factors that can affect the self-discharge battery characteristics. Batteries need to be periodically recharged to compensate for the self-discharge. The self-discharge rate of a battery is usually quantified in terms of a percentage loss of the capacity per month or per year, although other performance values are also sometimes used. The typical value of self-discharge rate of the lead-acid batteries at the room temperature is approximately 2–5%, up to 15–25% per month for aged batteries [37].

There is a considerable interest in studying the discharge parameters and the cycle lifetime of light weight conductive porous grids in the lead-acid batteries. Identifying the RVC-based lead-acid battery self-discharge characteristic is important for laboratory testing and practical applications. RVC is characterized by an open-pore structure, high-specific surface area and high void fraction [38]. In our previous papers, we have demonstrated cells employing positive plates with RVC grid electroplated with Pb (Pb/RVC grid) and negative ones based on Pb/RVC grids or bare RVC [39–41]. Early uses of RVC were largely restricted to small plates for lead-acid batteries; however, the obtained results were promising for the prototype two-plate 2-V cells with RVC covered with lead and a hybrid three-electrode lead-acid cell with one plate based on RVC [39–42].

In this paper, we describe the design, assembly, and battery tests of four-plate 2-V cells with positive and negative RVC-based grids. RVC coated with lead has been used as positive and negative plates' current collectors of the lead-acid cell. Cells used during our newest experiments have capacities up to ca. 46 Ah and we also present results for a complete 12 V battery. The aim of this work is a demonstration of construction and preliminary electrochemical performance of upscaled versions of RVC-based lead-acid cells, using multiple plates and having high discharge capacities. The Peukert's dependence of a lead-acid cell based on our own carbon material with conductivity higher than RVC is also presented. Additionally, we measured cycle life of a 2-V RVC-based cell, using improved charging algorithm compared to our previous work, as well as cycle life of a 12-V battery. Moreover, we present the self-discharge characteristic of a lead-acid cell with RVC-based collectors.

Material and methods

The RVC/Pb grid preparation

RVC with 20 p.p.i. (pores per inch) porosity grade, purchased from ERG Material and Aerospace Corporation, was chosen for this research, based on our previous results and considering its properties, such as low weight, porosity, and electrical conductivity. To prepare the RVC grids, the RVC was cut into pieces with dimensions ca. 118 mm × 100 mm × 5 mm (height × width × thickness). A cell used in cycle life measurement used smaller collectors: positive ones ca. 45 mm × 50 mm × 5 mm in size and negative with porosity 30 p.p.i. and size ca. 45 mm × 50 mm × 4 mm. One of the batteries (CPC cell) used small slabs of our own material, conductive porous carbon (CPC), instead of RVC [43]. They had dimensions of ca. 50 mm × 25 mm × 5 mm. In order to supply current to the porous carbon structure, a lug made of Pb was attached to the reticulated vitreous carbon slab. The RVC slabs were then electrodeposited with Pb. The electroplating process was conducted in a methanesulfonate bath with the RVC slabs as the cathode and Pb plate as the anode [44, 45]. The RVC slabs with thin (10 μm) layer of lead were used as the negative current collectors in a lead-acid battery and RVC slabs with thicker (100 μm) layer of lead as the positive ones. The thicknesses of the Pb layers were calculated from the real surface area of the RVC [38] and lead deposit weights. The surface morphology of the deposits was observed under a JEOL JSM-6490LV scanning electron microscope (SEM).

Plates preparation and cell assembly

The plates on the RVC-based collectors were prepared as per standard procedure for typical grid collectors. The RVC/Pb grid was made into positive and negative electrodes following the pasting and formation process. The respective paste was physically forced into the pores of the RVC/Pb slabs with a plastic spatula, and excess was scraped off of the surface. The battery pastes were common active masses used commercially by a battery manufacturer, with standard composition including expanders for negative plates and with addition of carbon fibers in the paste for positive plates. They contained 80% of

leady oxide. The nominal capacities of the negative and positive active masses were ca. 145 and ca. 120 Ah kg^{-1}, respectively. The pasted plates were cured at 45 °C, in a relative humidity of 90% for about 24 h, and then dried at 45 °C for the next 24 h. The amount of the negative paste in the typical RVC/Pb slab was ca. 190 g, and the electrode size (the dimensions of the coated part of the foam slab) was ca. 120 mm × 102 mm × 5.5 mm. For the positive electrode, the amount of positive paste and electrode size were ca. 180 g and ca. 121 mm × 103 mm × 5.5 mm, respectively. The cured plates (two positive and two negative) were separated with a PE envelope-type separator and were placed in a polypropylene container.

Figure 1 shows the overall process of preparing a complete four-plate 2-V cell with the RVC-based plates. We also constructed one 12-V battery, composed of six 2-V cells. The cells were similar to ones described earlier in this paragraph, with exception of having 30 p.p.i. RVC grids in negative plates. The cells were placed in a standard polypropylene casing, linked with electrical connectors, and sealed with a lid typical for flooded batteries. As for the RVC cell used for cycle life measurements, it was prepared from smaller RVC slabs and had only one positive and one negative plate.

Formation and testing of cells

The test cells were assembled with equal number of positive and negative plates per cell, thus the capacity was limited by the positive electrode. Using the Ah-equivalent of the nominal capacities of positive active masses, the total Ah-equivalent (C_n) was calculated, for a typical four-plate 2-V cell with the RVC grid C_n was equal to 43.1 Ah.

The formation of the plate was carried out in sulfuric acid as electrolyte with specific gravity of 1.14 g cm^{-3}, after soaking for 1 h. The formation was conducted at a constant current 0.067 C_n which corresponds to a number of Amp-hours equal to 485% of the nominal capacity within a time period of 70 h. After the formation the cell was filled with H_2SO_4 with specific gravity 1.28 g cm^{-3}, (electrochemical equivalent value is 133.0 Ah dm^{-3} [46]).

Formation and galvanostatic charge-discharge tests on the batteries were performed using Atlas 1361 battery tester. The testing of the cells was comprised of charging/discharging cycles with a depth of discharge (DoD) equal to 100%. The charge current used was 0.05 C_n (the 20-h rate) for 24 h and charging was assumed to be completed when the charge factor exceeded 120%. The charge factor corresponds to the percentage ratio between the ongoing number of charged Amp-hours and the previously obtained discharge capacity. Discharging of the cell was done using a constant current at the 20 h rate (0.05 C_n), 10 h rate (0.1 C_n), and 5 h rate (0.2 C_n), where the current rating is expressed using the nominal capacity of the cell (C_n), calculated for standard RVC cells at 43.1 Ah. The discharge cut-off voltage was 1.75 V. Measurements used for presenting Peukert's dependency used discharge currents from 0.05 C_n up to 3 C_n. Discharges with current rates 1 C_n and 3 C_n were continued until the voltage dropped below 1.6 V. Between each discharge/charge cycle presented in Peukert's dependency, there was a single discharge/charge cycle with 0.05 C_n rates.

The cycle life measurements for the 2-V cell were performed using 0.1 C_n charge and discharge rates. The cut-off voltage for discharge was 1.75 V. Charging was composed of three phases. First, the cell was charged with constant 0.1 C_n current until it reached 2.55 V. Then the voltage was kept constant at 2.55 V until current dropped to 0.02 C_n. Finally,

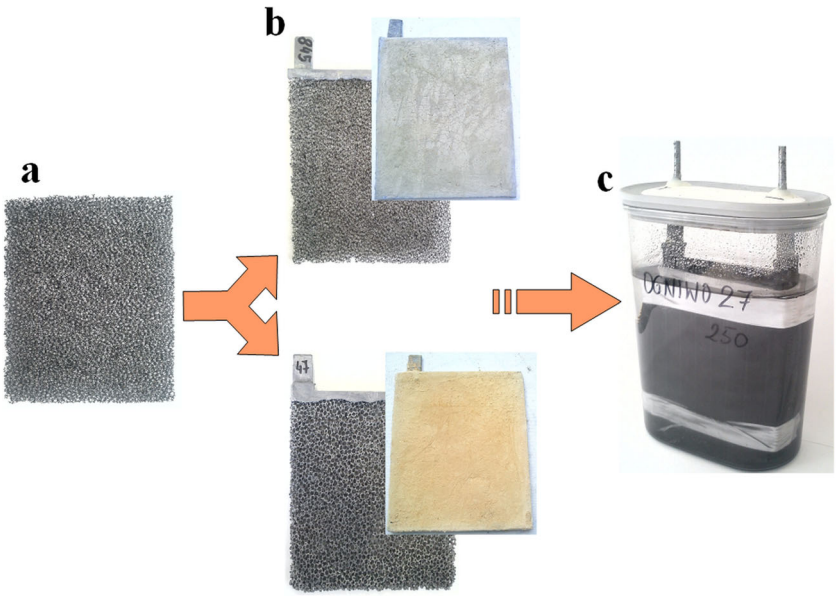

Fig. 1 Preparation of a 2-V RVC/Pb-based cell. **a** RVC slab, **b** electroplated electrodes, and pasted negative (upper part) and positive (lower part) plates **c** a complete 2-V cell

the cell was charged for 2 hours with constant current of 0.03 C_n.

The 12-V battery cycle life was tested by repeating the cycles of partial discharging and charging it afterwards. For each cycle, the battery was discharged for 1 h with a 0.25 C_n current. It was then charged for 155 min with a constant voltage of 14.8 V, and then for 5 min with a 0.125 C_n current. The voltage of the cell at the end of discharge was recorded and the measurement ended when it dropped below 10.5 V.

The self-discharge characteristics of the RVC-based lead-acid cell were assessed in this study by measuring the discharge voltages and capacities after storage for different time periods, when disconnected from any circuits. Since the open-circuit voltage (OCV) of the cell depends on the state of charge, the cell was fully charged before the storage in this investigation. The battery was charged at the 20 h rate for 24 h. After charging, the cell was disconnected for 1.5, 3, 6, and 12 months and after each time period a measurement of the open circuit potential and capacity loss at room temperature (25 °C) were conducted. First, the open circuit potential was measured and then the cell was discharged to 1.75 V cut-off voltage with a 0.05 C_n current. The cell was then charged for 24 h and then discharged again with 1.75 V cut-off voltage at a 0.05 C_n charge and discharge rates. The capacity loss was then determined from comparison of these two discharge capacities. All tests were conducted at room temperature. After experiments were finished, the total life of battery was almost 2 years (1.5 then 3 then 6 then 12 months).

Results and discussion

Surface morphology of the RVC/Pb

Figure 2a, b shows the surface morphology of the negative RVC-based collector.

Figure 2a presents the SEM image of the electroplated lead on reticulated vitreous carbon, in which the three-dimensional reticular structure of the RVC/Pb can be seen. Figure 2b shows a cross section of the RVC/Pb filament. The thickness of the lead coating was about 10 μm, which was in agreement with calculated thickness values of the lead layer on the base of Faraday's law. It can be seen from the images that the RVC is completely covered with lead coating and the electrodeposited lead has a good contact with the RVC. The surface of the lead coating is also uniform over the whole surface. Results obtained for large RVC collectors are similar to these achieved for smaller ones in our previous work [42].

The parameters of RVC/Pb electrode

The surface area is an important parameter for the current collector. The higher the specific surface area of RVC/Pb and the more effective contact between carbon and the active material, the higher the efficiency of the active material in charge generation due to battery reactions. RVC/Pb grids with Pb thickness 10 and 100 μm were used as negative and positive current collector, respectively. Generally, replacing a lead alloy grid with carbon foam allows to decrease the amount of lead used in battery by about 3 kg of Pb in 50-Ah battery, with specific energy equal to ca. 50 Wh kg^{-1}.

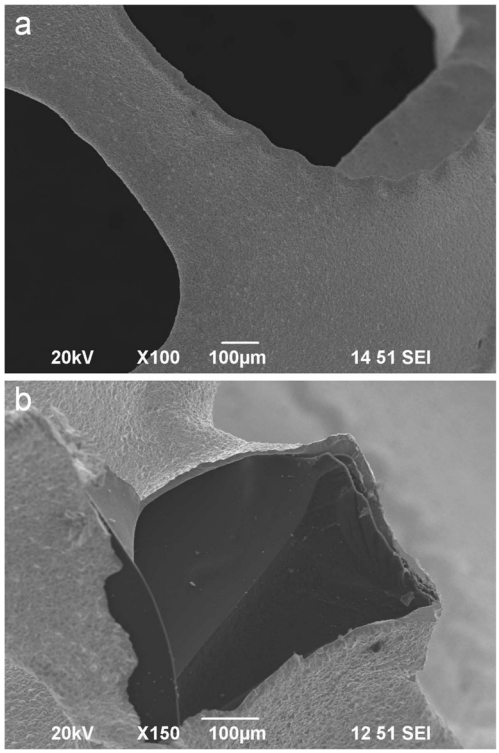

Fig. 2 SEM images of the negative RVC/Pb-based collector. **a** Surface morphology. **b** Filament cross section

The parameters such as the ratio of collector weight to electrode weight (α) and the ratio of the active mass to the collector surface area (γ) are normally used for efficiency evaluations and in plate design practice. The values of α and γ depend on the design of the plates. Generally, a smaller value of α parameter indicates a higher participation of the active mass in plate density capacity. Lower value of γ can lead to better active mass reactivity efficiency, but would also increase to the corrosion rate of the positive grid and a shorter cycle life [32, 46]. For SLI automobile lead-acid batteries, usually, the value of α varies between 0.35 and 0.60. The value of the γ parameter, especially for positive plates, is placed between 2 and 2.5 g cm^{-2} [46, 47]. The technical parameters of the high capacity negative and positive electrodes based on reticulated vitreous carbon (RVC) were estimated in Table 1.

The table shows the properties of the RVC-based plates of our new lead-acid battery such as the weight of their construction elements, the geometric and real surface area, and

Table 1 Parameters of negative and positive electrodes

Parameters	Negative electrode RVC/Pb10μm	Positive electrode RVC/Pb100μm
RVC grid mass [g]	2.5	2.6
Metal coated grid [g]	7.4	79.0
Electrical collector [g]	25.2	29.3
Collector RVC/Pb [g]	35.1	111.0
Equivalent mass of AM [g]	191.0	179.9
Total mass electrode [g]	226.1	290.8
Geometric area [cm^2]	122.4	124.6
Real surface area [cm^2]	692	722
α	0.155	0.382
γ [g/cm^2]	0.276	0.249

α, $M_{COLLECTOR}/(M_{AM}+M_{COLLECTOR})$; γ, $M_{AM}/S_{COLLECTOR}$; M_{AM}, the mass of the active material; $M_{COLLECTOR}$, the mass of the collector; $S_{COLLECTOR}$, the real surface area of collector

calculated α and γ coefficients of the RVC-based electrodes. The real surface area of RVC estimation was based on the data for reticulated vitreous carbon with 20 p.p.i. reported by producer [38]. By comparing the negative electrode RVC/Pb10μm with the positive RVC/Pb100μm, we can see that the negative one has a much lower mass. The reduction of the mass of the electrode is a result of a much thinner layer of lead and a lower weight of the coating. The α factor equals 0.16 for negative and 0.38 for positive RVC/Pb plates, respectively. Coefficient γ equals 0.28 g cm^{-2} for negative and 0.25 g cm^{-2} for positive plates and is much lower than for standard plates based on cast grids [40]. A small value of factors α and γ of the negative and positive electrodes based on RVC/Pb in comparison to classic lead-acid battery plates will improve the charge distribution efficiency in the active material due to 3D structure of RVC matrix. Generally in classic SLI lead-acid batteries, the charge densities of positive and negative active mass (PAM and NAM) is 120 and 145 Ah kg^{-1} respectively. In the new lead-acid battery based on RVC, the significant increase (ca. 20%) of the charge density in PAM and NAM was observed, up to 145 and 175 Ah kg^{-1} respectively [41]. This improvement is also a result of a highly developed interface area of active mass with carbon grid through the lead deposit. Due to higher specific surface area values, both the current collectors of the RVC/Pb10μm negative and RVC/Pb100μm positive electrodes reduce the density of the current passing through the contact surface, because RVC/Pb has a bigger contact area with the active material. As a result, the cell with RVC/Pb plates has high discharge voltages and discharge capacity. Therefore, the RVC/Pb current collector can improve the discharge performance of the lead-acid cell. Nevertheless, further study is still needed to improve the discharge performance of the cell. Optimization of the positive and negative plate construction and paste formulation are expected to yield better discharge performance of the RVC-based lead-acid cell in the future.

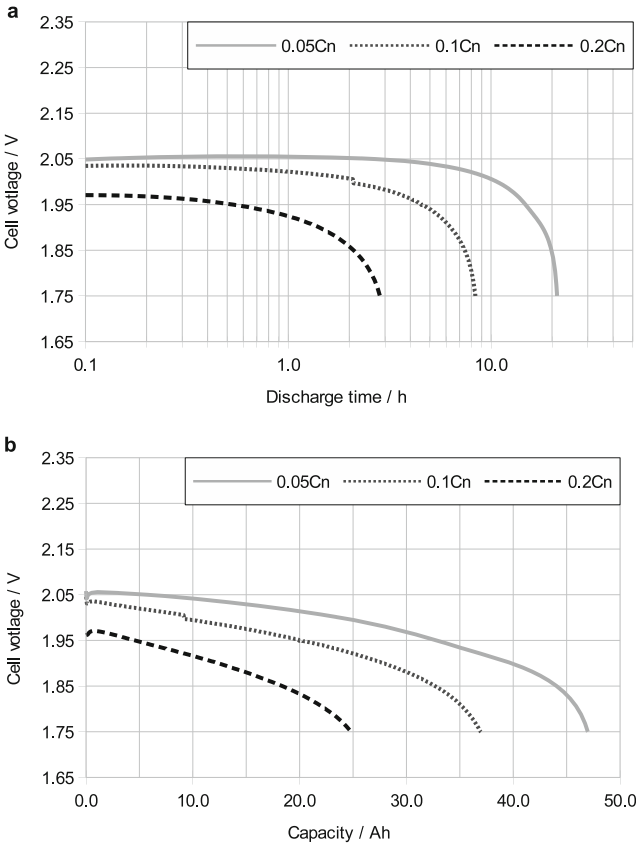

Fig. 3 Discharge performance characteristics of the lead-acid cell with RVC-based collectors at different rates, cell voltage is plotted versus discharge time (**a**) and discharge capacity (**b**)

Characteristic of the lead-acid cell with RVC/Pb plates

Table 2 presents the weight mass analysis of cells components. The component participation in total mass of constructed cell is enclosed in brackets.

Table 2 Weight analysis of the main constructing elements of the lead-acid cell on RVC-based

Negative collector RVC/Pb10μm	Negative active mass	Positive collector RVC/Pb100μm	Positive active mass	Separator	Electrolyte	Container	Top lead
70.2 g (2.9%)	382.0 g (15.7%)	221.9 g (9.1%)	359.7 g (14.7%)	9.7 g (0.4%)	1280.0 g (52.5%)	28.0 g (1.2%)	88.3 g (3.6%)

The data in Table 2 show the contribution of masses of negative and positive collectors to the total cell mass which are 2.9 and 9.1%, respectively. The proportion of total mass of the collectors to the total battery mass is approximately 12% in comparison to ca. 25–30% in batteries with standard cast grids [41]. The thickness of lead deposited on grid of negative and positive collectors have been optimized and it was the compromise between weight and durability during cycling of battery plates [39–42]. A certain thickness of lead coating for RVC is essential due to the corrosion of the positive plates during charge-discharge cycles. It was found that in the case of negative plates, the lead deposit on carbon is not necessary due to good chemical resistivity of carbon (RVC) with the NAM (mainly Pb powder) during charging-discharging processes [39, 40]. The thin layer of lead on carbon increases only the mechanical behavior-resistivity and current conductivity of electrode matrix. The cell was flooded with an excess of the electrolyte; therefore, the acid weight contribution is relatively high. The masses of container, top lead, and separator are a very low contribution to the total cell mass.

Initial performance of the lead-acid cells with RVC/Pb plates

After the end of formation process, the cells were subjected to three charge/discharge cycles at a 0.05 C_n rates in order to determine the capacity of the cell. The discharge and procedure was described in the "Formation and testing of cells" section. In the first cycles, the capacity of the cell varies between 105 and 109% of the calculated nominal capacity of the cell (43.2 Ah), which gives an average value of about 46 Ah. The average value shows that plates have been formed completely and the electrical capacity of active mass deposited on porous carbon (RVC) is higher in comparison to deposits on standard lead alloy grids.

Performance of the lead-acid cells during different discharging procedures

The charge-discharge test was performed using 0.05 C_n, 0.1 C_n, and 0.2 C_n discharge currents. The battery discharging and charging procedure has been described in detail in the "Formation and testing of cells" section. The cell capacity during the discharge cycle was limited by the positive electrode due to lower electrical density of PAM capacity (Ah kg^{-1}) in comparison to NAM.

Figure 3 shows the discharge performance at different rates of the 2-V lead-acid cell with RVC-based electrodes. Figure 3a presents the semilogarithmic plot of the cell voltage changes during the discharge. Figure 3b shows the dependence of cell voltage on its discharge capacity during discharging process at different discharge rates. At the lowest rates, cell voltage and capacity have the highest values. At

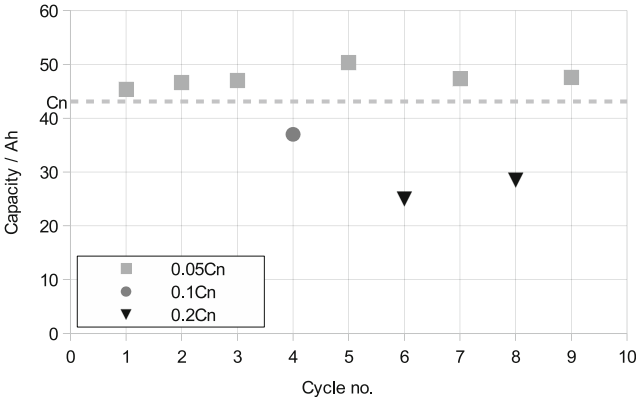

Fig. 4 Evolution of the initial discharge capacity during the cycling (cyclic work) of the lead-acid cell with RVC/Pb plates

0.05 C_n, 0.1 C_n, and 0.2 C_n discharge rates, the capacities of the cell in comparison to nominal capacity are 117, 86, and 58%, respectively. Figure 3a, b indicates that higher drain rates result in the reduction of the cell voltage and capacity. This effect is typical for all kind of batteries, also for classical SLI lead-acid batteries, the difference between battery capacity with the decreasing rate discharge from 0.2 C_n to 0.05 C_n is similar. It has to be noted that thickness of plates used in new batteries is three–four times higher (5–6 mm) in comparison to traditional lead-acid battery and the expected overpotential connected with the concentration polarization should grater but the charge distribution efficiency in the active material due to 3D structure of RVC matrix compensate this effect.

Figure 4 shows the changes in capacity of the lead-acid cells with RVC/Pb grids during first nine cycles with different rates of discharging. After the first three cycles at discharging rate at 0.05 C_n, the fourth discharging rate was taken at 0.1 C_n. The average cell capacity calculated from these first three cycles was ca. 46 Ah. The cell capacity during the fourth cycle with higher discharge rate of 0.1 C_n was 37 Ah. It is interesting that capacity of the cell determined in the fifth cycle at discharging current 0.05 C_n exceeded 50 Ah (50.3 Ah) which means that during the fourth cycle some reorganizations inside

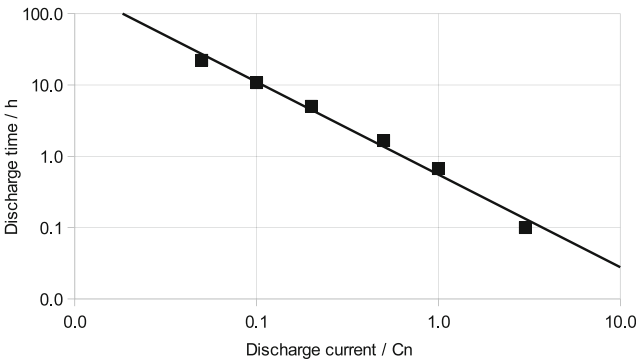

Fig. 5 Peukert's dependency for a 2-V CPC-based cell, nominal capacity 2.2 Ah

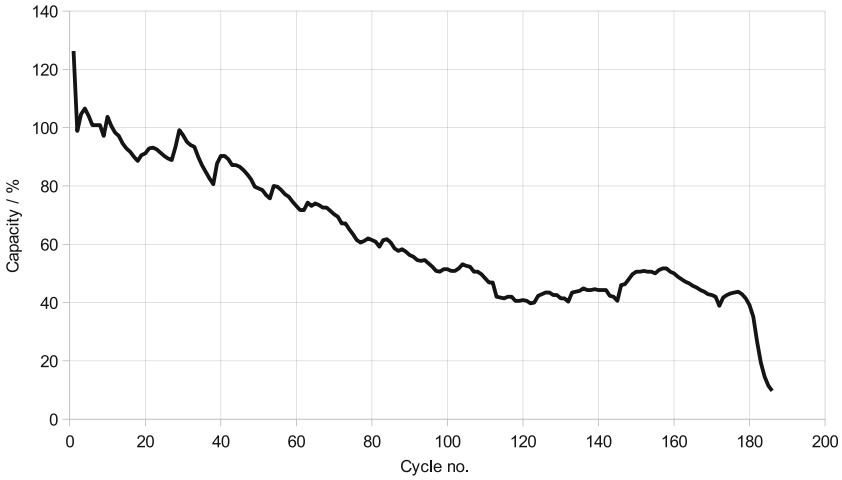

Fig. 6 Cycle life of a small 2-V RVC/Pb-based cell, nominal capacity 3.4 Ah

active mass take part—these are the continuation of the formation process. The sixth and eighth discharges were taken at higher 0.2 C_n rate and calculated cell capacity was 25.0 and 28.5 Ah respectively. Every time after returning to lower discharging rates at 0.05 C_n, the cell capacity was close to average value after the first three cycles. It can be seen from all the cycling sets that the cell performs well with a good cycling stability and its capacity was relatively high. The largest discharge capacity of the cell was 50.3 Ah (116%) at 20 h discharge rates. The capacity was ca. 45.4 Ah initially, and ca. 46.7 at the end of the ninth cycle at 0.05 C_n discharge rates. The cell capacity during the initial cycles does not change significantly.

The discharge performance of a cell based on CPC material was also tested. It was a smaller cell, with nominal capacity of 2.2 Ah.

In Fig. 5 Peukert's dependency for the CPC cell is shown. It reached 107% of nominal capacity during 0.1 C_n discharge, 67% for 1 C_n discharge and 30% for 3 C_n discharge. These results are an improvement over the RVC cells and are similar to values obtained by good lead grid-based batteries. This increase in the capacity is a consequence of better conductivity of the used carbon material, CPC. From the obtained results, a parameter n was calculated, according to Peukert's equation $K = I^n t$, where I is the discharge current, t is the discharge time and K and n are empiric constants. The calculated value of n is equal to 1.30, which shows that cells with reticulated carbon collectors even during high-current discharge can reach similar capacities as standard lead-acid batteries. The n parameter for lead-acid batteries is usually between 1.1–1.4 [48] and even for modern constructions it stays in 1.25–1.30 range [49, 50].

The cycle life of a 2-V cell and a 12-V battery with RVC/Pb-based cells

Figure 6 shows the cycle life of a smaller cell with RVC/Pb grids. The nominal capacity of this cell was 3.4 Ah.

This cell had initial capacity exceeding the nominal one, reaching even 130%. As expected for lead-acid cells, the capacity was gradually decreasing with the number of completed cycles. It finished almost 200 cycles before failure, when

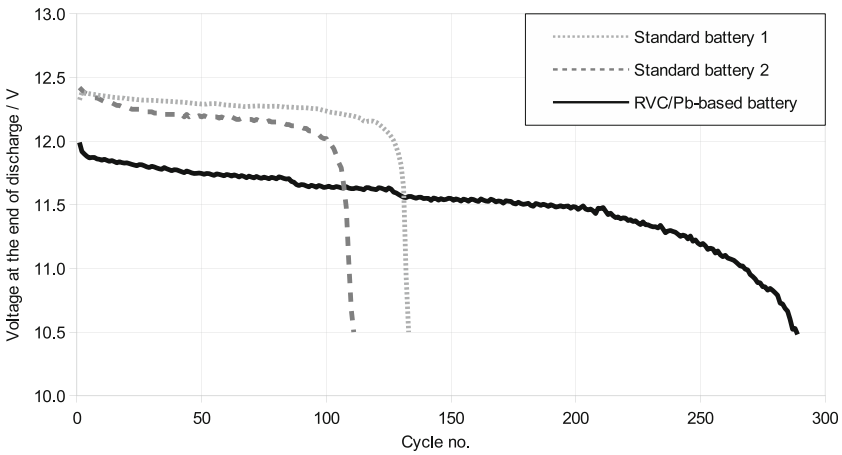

Fig. 7 Cycle life during partial discharge of a RVC/Pb-based 12-V battery compared to standard 12-V batteries

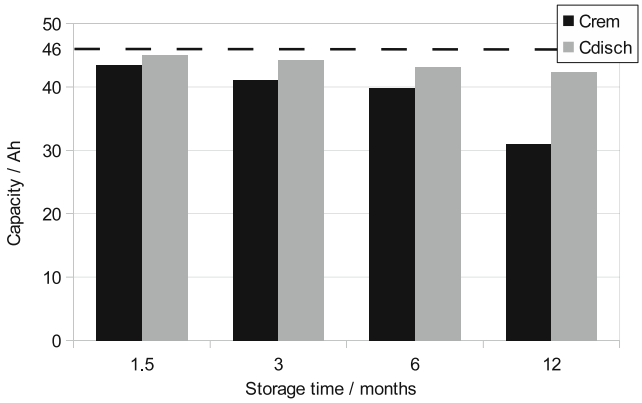

Fig. 8 Evolution of capacity after a different period of storage of a lead-acid cell with RVC/Pb plates (the dashed line shows the initial capacity at 46 Ah)

the capacity dropped rapidly below 10%. The final capacity drop was probably caused by the corrosion of lead electrodeposited on the carbon collectors in positive plates. Nevertheless, this result shows that the cell with the RVC/Pb grids can complete many charge/discharge cycles and is comparable in this regard to characteristics of standard lead-acid cells.

The cycle life of a complete 12-V battery was tested according to procedure described in the "Formation and testing of cells" section. It has to be noted that two kinds of batteries (commercial and RVC/Pb) with active masses from the same source were tested. The results obtained by RVC/Pb battery compared to two typical, commercial lead-acid batteries are shown in Fig. 7.

RVC/Pb-based battery completed 289 cycles and two different commercial batteries completed 67 and 111 cycles (average 89 cycles). The results for partial discharge cycles for the battery of a new type are very good, its characteristic is much better than for commercial ones. The result for the RVC/Pb battery is also a significant improvement in battery performance over the full discharge/charge cycles. The charging voltage constraint of 14.8 V (2.47 V per cell) limits the ability to fully charge the RVC/Pb battery, but on the other hand, it slows down the corrosion of a protective Pb layer on positive current collectors, which is the main reason of failure of this battery type. Longer cycle life can be explained by improved electrical contact between the active mass and the reticulated collector, which improves the conductivity of the discharged material. Additionally, the 3D structure of our collector provides better mechanical support, compared to a standard grid, which prevents excessive shedding of the active mass. The measurement's results show that the 12-V battery constructed from 2-V RVC/Pb cells retains their good electrochemical characteristics.

Self-discharge and capacity losses of the lead-acid cells with RVC/Pb plates

Capacity loss during charge-discharge cycling and storage time (shelf time) are major parameters, which inform about the life of a battery. The self-discharge and capacity losses of the RVC-based lead-acid cell have been investigated at different storage times (0, 1.5, 3, 6, and 12 months). In the end, the battery was tested continuously for ca. 2 years. It is a very important additional information about the durability of our new carbon lead-acid cells. The open circuit voltages (OCV) and capacity losses of the cell were measured as a function of different time period storage at the standby mode. The capacity loss is calculated by dividing the capacity remaining after storage by the capacity of the same cell recharged in the next cycle.

$$\text{Capacity loss}(\%) = \frac{C_{\text{disch}} - C_{\text{rem}}}{C_{\text{disch}}} \cdot 100\% \quad (1)$$

where C_{rem} is the capacity during the first discharge after storage at 0.05 C_n rate and C_{disch} is the capacity during the second discharge at the same rate after recharging the cell. The

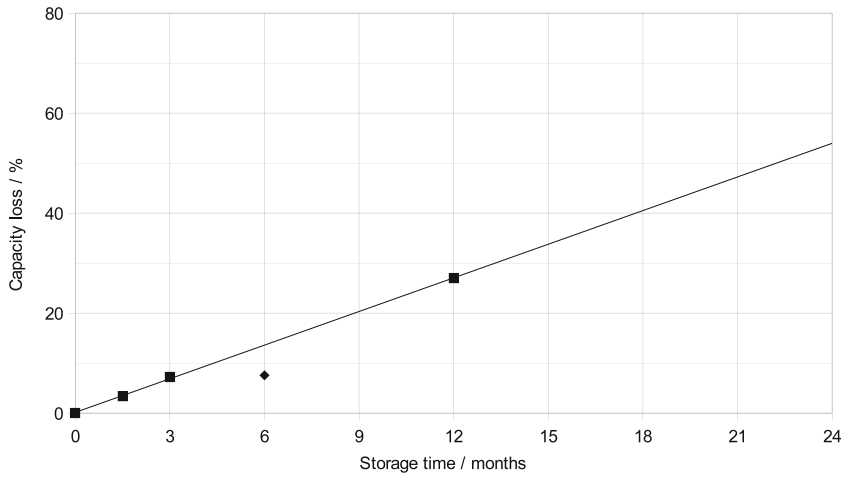

Fig. 9 Capacity loss of the lead-acid cell with RVC/Pb collectors as a function of storage time at 25 °C (the 6-month point is excluded from the trend line)

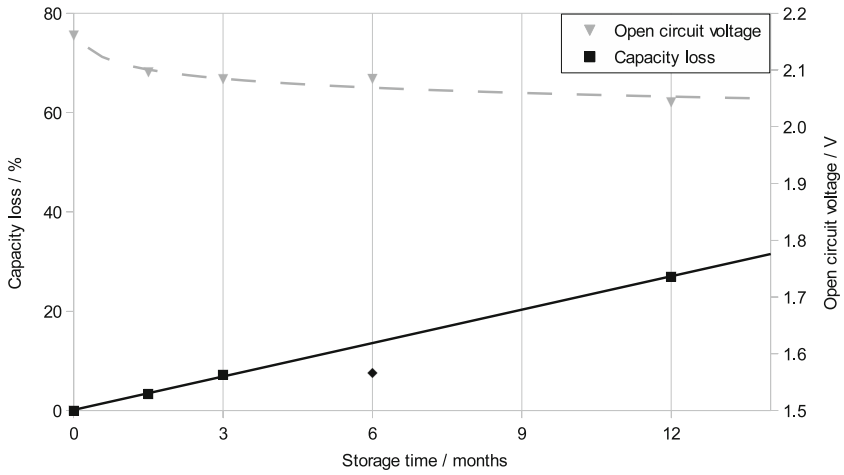

Fig. 10 Open circuit voltage and capacity loss as functions of storage time

charging procedure has been described in the "Formation and testing of cells" section. Figure 8 shows the remaining capacities and discharge capacities of the lead-acid cell with RVC/Pb plates after storage for different times.

As a result of the experiment, after 1.5 months of open-circuit storage, the capacity loss of the cell is approximately 3%. After storage for 3 and 6 months, the capacity loss is almost the same with value of approximately 7%. The capacity loss increases to 28% after storage for 12 months. Long periods of open-circuit stand can result in water loss and sulfated plates, leading to an increase in self-discharge. It has to be noted that total time of all experiments with one battery took almost 24 months (including the initial testing and the sum of self-discharge tests taking 1.5, 3, 6, and 12 months) and its capacity has dropped from 46 (fresh battery) to 42.5 Ah (end of the experiments). It means that loss of the initial capacity after 2 years of battery storage is no more than 10%.

Figure 9 shows the capacity loss of the RVC-based lead-acid cell after various storage times at 25 °C.

The remaining capacity of the cell has an almost linear dependence with the storage time. It can be seen from Fig. 9 that after extrapolation, the storage time required to reach half of the initial capacity of the cell (after the activation by charge-discharge cycling) exceeds 22 months, i.e., monthly capacity loss for a carbon-based lead-acid battery at open circuit is about 2.3%. At 25 °C, the remaining capacity of the lead-acid cell with RVC/Pb plates is reduced to 60% of initial capacity after 18 months of storage, while the remaining capacity of a conventional lead-acid cell is reduced to this value in much shorter time, even as low as 8 months for 5% capacity loss per month [37, 51].

Figure 10 shows plots of the capacity loss and the open circuit voltage versus storage time for the lead-acid cells with RVC/Pb plates.

It can be seen that open circuit voltage (OCV) is decreasing rather fast in the beginning but then slows down for longer storage times. Initially, the OCV rapidly decreased from 2.15

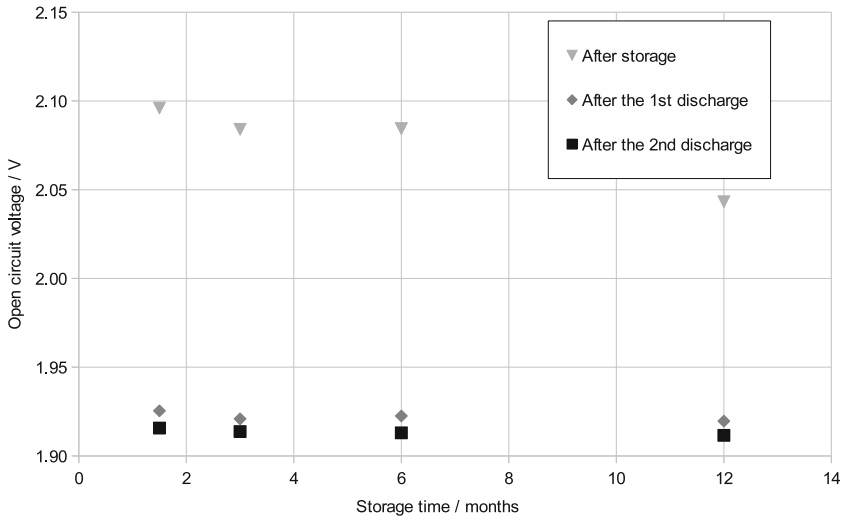

Fig. 11 A plot of the open circuit voltage after the storage and after two discharges versus the storage time period of a RVC-based cell

Table 3 Self discharge measurement and capacity degradation after standby and after the activation by charge-discharge cycling

Storage time in months (days)	The open circuit potential [V]	Discharge at a 0.05 C_n [Ah]		Capacity loss [%]	Capacity degradation rate[a] [Ah per day]
		remaining capacity (C_{rem})	discharge capacity (C_{disch})		
1.5 (45)	2.096	43.5	45.0	3.33	0.033
3 (90)	2.084	41.1	44.3	7.22	0.036
6 (180)	2.084	39.9	43.1	7.42	0.018
12 (360)	2.043	30.3	42.4	28.5	0.034

[a] The capacity degradation rate is defined as the capacity change ($C_{disch} - C_{rem}$) divided by storage time

to 2.10 V, as shown in Fig. 7. The voltage drop becomes much slower after the 3-month storage and its rate becomes relatively steady (ca. 2.05 V) for longer standby periods. We suspect that the initial fast drop of the OCV is caused by relatively high area of our collector and shorter path from bulk of the active mass to the conductive matrix, which allows for quicker reactions with active mass and electrolyte and passivation of the grid. We think that above processes cause faster stabilization of the active masses during the first cycles, which is visible in the initial OCV drop.

Figure 11 shows the comparison of the open circuit voltages immediately after the storage and voltage measured after two discharge tests.

The OCV for discharge tests was registered after the first discharge after storage and after the discharge of the recharged cell (the second discharge). It is clear from Fig. 11 that the OCV after the cell was subjected to discharge at 0.05 C_n rate is lower by approximately 0.2 V than OCV after storage. The cell voltages after discharge tests are relatively steady at all time periods of storage, but OCV of the cell after discharge following the recharging is lower than OCV after discharge and immediately after storage. Additionally, the values of the open circuit voltages after the two discharge tests follow the same pattern for different storage times.

The values of the open circuit potential, different discharge capacity, capacity loss, and capacity degradation of the cell after different storage times are summarized in Table 3.

From this table, we can see that capacity degradation is similar for storage period of 1.5, 3, and 12 months. Average capacity degradation of the cell is 0.034 Ah per day. The rate at which lead-acid cells with RVC/Pb plates loses its capacity in open circuit conditions is around 2.3% per month. This result shows that an improved design of the lead-acid cell with the use of RVC/Pb as current collectors significantly reduces the cell self-discharge rate.

Conclusions

An innovative, complete four-plate 2-V cell with the RVC grids and high capacity of 46 Ah was demonstrated. RVC coated with lead has been used as current collectors for positive and negative plates of lead-acid cell. The electrodeposited lead coating had thicknesses of approximately 10 and 100 μm (for negative and for positive plate, respectively) and good contact with the RVC. The RVC/Pb grids had bigger specific surface area and bigger contact area with the active material, compared with cast grids. Small factors α and γ of the negative and positive RVC/Pb-based electrodes indicate that the capacity of the RVC/Pb electrodes and utilization efficiency of the active material is improved. RVC/Pb plates are characterized by low contribution of masses of the collectors to the total cell mass in comparison to standard cast grids. A complete, 12-V battery was also constructed from similar cells. The galvanostatic charge-discharge and self-discharge characteristics of the four-plate 2-V cells with the RVC grids were investigated. Performance of the lead-acid cells with RVC/Pb plates at different discharge regimes shows that the cell has a high discharge voltages and discharge capacity. At 0.05 C_n, 0.1 C_n, and 0.2 C_n discharge rates, the capacities of the cell are 117, 86, and 58% of the nominal capacity, respectively. The performance during high-current discharge can be improved by usage of better conducting carbon materials, like CPC. The CPC-based cell reached 67% capacity for 1 C_n and 30% for 3 C_n discharge. Its n parameter in Peukert's equation is equal to 1.30, a value very similar to standard lead-acid batteries. During the tests of the cycle life, a cell with RVC/Pb plates completed almost 200 full discharge/charge cycles, which is comparable to results of a standard grid-based battery. The cycle life of a 12-V battery with the RVC/Pb collectors was also tested during partial discharge cycles. The new type of battery completed almost 300 cycles compared to around 100 cycles by standard batteries. The capacity loss during storage for the cell has an average value of 0.034 Ah per day or 2.3% of initial capacity per month. This result indicates that RVC/Pb as current collectors potentially reduces the cell self-discharge rate. Obtained results show that the new construction of the lead-acid cell with RVC/Pb plates can improve the performance during discharge and also reduce the self-discharge of the battery. The new type of lead-acid cell additionally shows promising results in regard to the cycle life. As a result of mentioned characteristics, the batteries with

reticulated current collectors should be suitable for the systems of energy storage generated by alternative sources of energy and electric and hybrid vehicles.

Acknowledgements Special thanks are due to Daramic LLC for providing battery separators for the research. This work was supported by the Global GMP Innovation Center.

References

1. The Worldwide rechargeable Battery Market 2011–2025. (2012) Avicenne Energy
2. Jung J, Zhang L, Zhang J (2016) Lead-acid battery technologies: fundamentals, materials, and applications. CRC Press, Boca Raton
3. Linden D, Reddy T (2001) Handbook of batteries, 3rd edn. McGraw-Hill Professional, New York
4. Czerwiński A (1995) Sposób galwanicznego nanoszenia ołowiu lub tlenku ołowiowego na przewodzące materiały węglowe. Patent RP 167796
5. Żelazowska M, Czerwiński A (1996) Materials of lead acid batteries LABAT 1996 conference: 107–110. Varna
6. Czerwiński A, Żelazowska M (2000) Elektroda z ołowiu lub z tlenku ołowiu. Patent RP 178258
7. Czerwiński A, Żelazowska M (2001) Akumulator ołowiowy. Patent RP 180939
8. Czerwiński A, Żelazowska M (1996) Electrochemical behavior of lead deposited on reticulated vitreous carbon. J Electroanal Chem 410(1):55–60
9. Czerwiński A, Żelazowska M (1997) Electrochemical behavior of lead dioxide deposited on reticulated vitreous carbon (RVC). J Power Sources 64(1–2):29–34
10. Czerwiński A, Rogulski Z, Obrębowski S, Siwek H, Paleska I, Chotkowski M, Łukaszewski M (2009) RVC as new carbon material for batteries. J Appl Electrochem 39(5):559–567
11. Wróbel J, Wróbel K, Lach J, Dłubak J, Podsadni P, Rogulski Z, Paleska I, Czerwiński A (2014) Zastosowanie usieciowanego węgła szklistego w elektrochemicznych źródłach prądu. Przem Chem 93: 331–338
12. Paleska I, Pruszkowska-Drachal R, Kotowski J, Rogulski Z, Milewski JD, Czerwiński A (2004) Electrochemical behavior of barium metaplumbate as a lead carrier. J Power Sources 129(2): 326–329
13. Żelazowska-Zakrent M (1998) Elektrochemia ołowiu i tlenku ołowiu (IV) osadzonych na porowatym węglu szklistym. Ph.D. dissertation, Warsaw University
14. Das K, Mondal A (1995) Discharge behavior of electro-deposited lead and lead dioxide electrodes on carbon in aqueous sulfuric acid. J Power Sources 55(2):251–254
15. Snaper A (2000) Electrochemical battery structure and method. Patent US 6060198
16. Gyenge E, Jung J (2003) Current collector structure and methods to improve the performance of a lead-acid battery. Patent WO 2003028130A1
17. Gyenge E, Jung J, Splinter S, Snaper A (2002) High specific surface area, reticulated current collectors for lead–acid batteries. J Appl Electrochem 32(3):287–295
18. Gyenge E, Jung J, Mahato B (2003) Electroplated reticulated vitreous carbon current collectors for lead–acid batteries: opportunities and challenges. J Power Sources 113(2):388–395
19. Gyenge E, Jung J, Snaper A (2006) Current collector structure and methods to improve the performance of a lead-acid battery. Patent US 7060391
20. Jang YI, Dudney NJ, Tiegs TN, Klett JW (2006) Evaluation of the electrochemical stability of graphite foams as current collectors for lead-acid batteries. J Power Sources 161(2):1392–1399
21. Chen Y, Chen BZ, Shi XC, Xu H, Shang W, Yuan Y, Xiao LP (2008) Preparation and electrochemical properties of pitch-based carbon foam as current collectors for lead-acid batteries. Electrochim Acta 53(5):2245–2249
22. Chen Y, Chen BZ, Ma LW, Yuan Y (2008) Effect of carbon foams as negative current collectors on partial-state-of-charge performance of lead-acid batteries. Electrochem Commun 10(7):1064–1066
23. Chen Y, Chen BZ, Ma LW, Yuan Y (2008) Influence of pitch-based carbon foam current collectors on the electrochemical properties of lead-acid battery negative electrodes. J Appl Electrochem 38(10): 1409–1413
24. Ma LW, Chen BZ, Chen Y, Yuan Y (2009) Pitch-based carbon foam electrodeposited with lead as positive current collectors for lead-acid batteries. J Appl Electrochem 39(9):1609–1615
25. Kelley KC, Votoupal JJ (2005) Battery including carbon foam current collectors. Patent US 6979513
26. Kelley KC, Ostermeier CF, Maroon MJ (2006) Composite material and current collector for battery. Patent US 7033703
27. Kelley KC, Ostermeier CF, Maroon MJ (2008) Battery having carbon foam current collector. Patent US 7341806
28. Kirchev A, Kircheva N, Perrin M (2011) Carbon honeycomb grids for advanced lead-acid batteries. Part I: proof of concept. J Power Sources 196(20):8773–8788
29. Kirchev A, Dumenil S, Alias M, Christin R, de Mascarel A, Perrin M (2015) Carbon honeycomb grids for advanced lead-acid batteries. Part II: operation of the negative plates. J Power Sources 279: 809–824
30. Kirchev A, Serra L, Dumenil S, Brichard G, Alias M, Jammet B, Vinit L (2015) Carbon honeycomb grids for advanced lead-acid batteries. Part III: technology scale-up. J Power Sources 299:324–333
31. Tabaatabaai SM, Rahmanifar MS, Mousavi SA, Shekofteh S, Khonsari J, Oweisi A, Hejabi M, Tabrizi H, Shirzadi S, Cheraghi B (2006) Lead-acid batteries with foam grids. J Power Sources 158(2):879–884
32. Dai CS, Zhang B, Wang DL, Yi TF, Hu XG (2006) Preparation and performance of lead foam grid for negative electrode of VRLA battery. Mater Chem Phys 99(2-3):431–436
33. Dai C, Yi T, Wang D, Hu X (2006) Effects of lead-foam grids on performance of VRLA battery. J Power Sources 158(2):885–890
34. Ji K, Xu C, Zhao H, Dai Z (2014) Electrodeposited lead-foam grids on copper-foam substrates as positive current collectors for lead-acid batteries. J Power Sources 248:307–316
35. Gladstone JH, Tribe A (1882) The chemistry of the Plante and Faure accumulators. J Frankl Inst 114(3):219–233
36. Rüetschi P, Angstadt RT (1958) Self-discharge reactions in lead-acid batteries. J Electrochem Soc 105(10):555–563
37. Garche J, Dyer CK, Moseley PT, Ogumi Z, Rand DAJ, Scrosati B (2009) Encyclopedia of electrochemical power sources. Elsevier, Amsterdam
38. Surface Area of Duocel® Foam, ERG Aerospace Corp. http://ergaerospace.com/technical-data/surface-area-of-duocel-foam/ Accessed 31 Jan 2018

39. Czerwiński A, Obrębowski S, Kotowski J, Rogulski Z, Skowroński JM, Bajsert M, Przystałowski M, Buczkowska-Biniecka M, Jankowska E, Baraniak M, Rotnicki J, Kopczyk M (2010) Electrochemical behavior of negative electrode of lead-acid cells based on reticulated vitreous carbon carrier. J Power Sources 195(22):7524–7529
40. Czerwiński A, Obrębowski S, Kotowski J, Rogulski Z, Skowroński J, Bajstert M, Przystałowski M, Buczkowska-Biniecka M, Jankowska E, Baraniak M, Rotnicki J, Kopczyk M (2010) Hybrid lead-acid battery with reticulated vitreous carbon as a carrier- and current-collector of negative plate. J Power Sources 195(22):7530–7534
41. Czerwiński A, Obrębowski S, Rogulski Z (2012) New high-energy lead-acid battery with reticulated vitreous carbon as a carrier and current collector. J Power Sources 198:378–382
42. Czerwiński A, Rogulski Z, Obrębowski S, Lach J, Wróbel K, Wróbel J (2014) Positive plate for carbon lead-acid battery. Int J Electrochem Sci 9:4826–4839
43. Bystrzejewski M, Podsadni P, Rogulski Z, Czerwiński A (2017) Sposób wytwarzania kształtek z porowatego wegla przewodzącego o określonej geometrii i porowatości. Patent application RP P423254
44. Czerwiński A, Rogulski Z, Wróbel K, Wróbel J, Lach J, Bajsert M, Przystałowski M, Kopczyk M (2014) Kolektor prądowy elektrod akumulatora ołowiowo-kwasowego, sposób jego otrzymywania oraz akumulator ołowiowo-kwasowy. Patent application RP P.408085
45. Czerwiński A, Rogulski Z, Wróbel K, Wróbel J, Lach J, Bajsert M, Przystałowski M, Kopczyk M (2014) Sposób wprowadzania masy czynnej do kolektora elektrod akumulatora ołowiowo-kwasowego. Patent application RP P.409464
46. Pavlov D (1995) A theory of the grid/positive active-mass (PAM) interface and possible methods to improve PAM utilization and cycle life of lead/acid batteries. J Power Sources 53(1):9–21
47. Pavlov D (2011) Lead-acid batteries science and technology. Elsevier, Amsterdam
48. Cugnet M, Dubarry M, Liaw BY (2010) Peukert's law of a lead-acid battery simulated by a mathematical model. ECS Trans 25: 223–233
49. Lannelongue J, Cugnet M, Guillet N, Kirchev A (2017) Electrochemistry of thin-plate lead-carbon batteries employing alternative current collectors. J Power Sources 352:194–207
50. Pavlov P, Rogachev T, Nikolov P, Petkova G (2009) Mechanism of action of electrochemically active carbons on the processes that take place at the negative plates of lead-acid batteries. J Power Sources 191(1):58–75
51. Crompton TR (2000) Battery reference book, third edn. Newnes, Oxford